



**HAL**  
open science

# Rosin natural terpenes as processing aid for polyhydroxyalkanoate: Thermal, mechanical, and viscoelastic properties

Gaëtan Charon, Jorge Peixinho, Laurent Michely, Alain Guinault, Valérie Langlois

## ► To cite this version:

Gaëtan Charon, Jorge Peixinho, Laurent Michely, Alain Guinault, Valérie Langlois. Rosin natural terpenes as processing aid for polyhydroxyalkanoate: Thermal, mechanical, and viscoelastic properties. *Journal of Applied Polymer Science*, 2022, 139 (43), 10.1002/app.53052 . hal-03816621

**HAL Id: hal-03816621**

**<https://hal.science/hal-03816621v1>**

Submitted on 1 Dec 2022



**HAL** is a multi-disciplinary open access archive for the deposit and dissemination of scientific research documents, whether they are published or not. The documents may come from teaching and research institutions in France or abroad, or from public or private research centers.

L'archive ouverte pluridisciplinaire **HAL**, est destinée au dépôt et à la diffusion de documents scientifiques de niveau recherche, publiés ou non, émanant des établissements d'enseignement et de recherche français ou étrangers, des laboratoires publics ou privés.



Distributed under a Creative Commons Attribution - NonCommercial 4.0 International License

# Rosin natural terpenes as processing aid for polyhydroxyalkanoate: Thermal, mechanical, and viscoelastic properties

Gaëtan Charon<sup>1</sup> | Jorge Peixinho<sup>1</sup>  | Laurent Michely<sup>1</sup>  | Alain Guinault<sup>2</sup> | Valérie Langlois<sup>2</sup>

<sup>1</sup>Laboratoire PIMM, CNRS, Arts et Métiers Institute of Technology, Cnam, HESAM Université, Paris, France

<sup>2</sup>Université Paris Est Creteil, CNRS, ICMPE, Créteil, France

## Correspondence

Jorge Peixinho, Laboratoire PIMM, CNRS, Arts et Métiers Institute of Technology, Cnam, HESAM Université, 75013 Paris, France.

Email: [jorge.peixinho@cnrs.fr](mailto:jorge.peixinho@cnrs.fr)

## Funding information

ANR PRCI SEABIOP

## Abstract

Rosin natural terpene (Dertoline) is compounded with a bacterial thermoplastic polyesters polyhydroxyalkanoate (PHA), specifically here poly(3-hydroxybutyrate) (PHB), a biodegradable and biocompatible polymer. The compatibility of the blend is examined with differential scanning calorimetry and thermal gravimetry analysis. In the range of concentration of Dertoline, from 5 to 15 wt%, a cold crystallization peak first shifts to slightly higher then lower temperature. Dynamical mechanical analysis and tensile tests confirm that the addition of Dertoline slightly decreases the elastic modulus. The degree of crystallinity again increases then decreases with the content of Dertoline. Polarized light microscopy reveals smaller diameter spherulites for PHB/Dertoline blends and their presence is discussed in relation to tensile tests. Overall, the addition of Dertoline has limited effects on mechanical properties of the blends: the stress at break and the strain at break. In addition, oscillatory rheology at different temperatures provides the activation energies and the parameters of a generalized Maxwell model. The temperature dependence of the rheological properties follows an Arrhenius form. Finally, transient step viscosity measurements are used in order to quantify the PHB thermal degradation.

## KEYWORDS

biopolymers and renewable polymers, differential scanning calorimetry, mechanical properties, packaging, rheology

## 1 | INTRODUCTION

The rapid increase of worldwide plastic accumulation in the environment calls for the reduction of conventional (petroleum-based) materials use and the development of alternative biodegradable plastics. In addition, the transition toward a zero-carbon footprint society requires to

reduce our reliance on fossil feedstocks. In this context, the biobased, compostable and marine biodegradable polymers blends need to be further understood in order to be regarded as serious alternatives on the plastic market.

Among the biobased and biodegradable polymers available, polyhydroxyalkanoates (PHAs) are remarkable because these are directly biosynthesized by bacteria.<sup>1-3</sup>

This is an open access article under the terms of the [Creative Commons Attribution-NonCommercial](https://creativecommons.org/licenses/by-nc/4.0/) License, which permits use, distribution and reproduction in any medium, provided the original work is properly cited and is not used for commercial purposes.

© 2022 The Authors. *Journal of Applied Polymer Science* published by Wiley Periodicals LLC.

Depending on the bacteria specificities and the carbon sources, different PHAs can be produced. According to their number of carbon atoms in the side chains, PHAs can be classified into different groups. Short chain length PHAs (scl-PHAs) are polyesters composed of monomers with 3–5 carbons, while medium chain length (mcl-PHAs) and long chain length (lcl-PHAs) have 6–14 carbons and over. The most well-know PHA is the poly(3-hydroxybutyrate) (PHB). These biobased polyesters present high biodegradability in various environments<sup>4–8</sup> and interesting biocompatibility.<sup>9–11</sup> Although these remarkable properties are appreciated, several drawbacks still limit PHB applications.

The mechanical, that is, the Young modulus (about 1 GPa) and the tensile strength (about 10 MPa), are comparable to usual plastics. However, the processing is considered complex because of the high thermodependency of the melt flow properties.<sup>12</sup> Moreover, the elongation required to break is poor.<sup>13</sup> Hence, neat PHB is considered as brittle and difficult to process.

To improve low ductility and low resistance to thermal degradation which leads to a narrow processability window, many efforts have focused on alternative strategies on the blends with plasticizers capable of improving their thermal and mechanical properties. Plasticizers offer the opportunities to reduce the degree of crystallinity and to improve the flexibility and the elongation of the material. Those plasticizers include aliphatic and aromatic compounds, vegetable oils and fatty acids, alcohols and polymers.<sup>14–18</sup>

Terpenes such as linalool, geraniol, and geranyl acetate were recently compounded with PHB to assess the influence of the content of these biobased molecules on the structural and mechanical properties of PHB.<sup>19</sup> The effect is more important with geranyl acetate with an improvement of the elongation at break. In this context, natural wood rosin can act as a source of antibacterial activity and also as chemical compatibilizer due to its chemically active structure that is rich in functionality.<sup>20</sup> Rosin blended with polylactic acid (PLA) have been reported to have successfully antibacterial properties.<sup>21</sup> The blending of PLA with gum rosin and ester of gum rosin was recently investigated<sup>22,23</sup> showing that they also have a lubricating effect. In order to get further insight for the processing aid of terpenes on PHB, additional data are required about the thermal behavior and crystallinity of the blend.

In the present investigation, rosin natural terpene, Dertoline, is tested with emphases on thermal, morphology and mechanical properties. Specifically, the thermal properties at elevated temperature in terms of viscoelastic behavior and transient viscosity are quantified in order to provide data for numerical simulations, which could be

used to predict melt flow in injection molding, micro-screw extrusion or fused deposition modeling.

## 2 | EXPERIMENTAL SECTION

### 2.1 | Materials

The biodegradable polymer powder PHB used in this investigation was produced by Biomer (Germany) as Batch T19. All polymer samples were stored in a room at 25°C in an aluminum closed bag protected from the air. Before any test, the PHB powder was dried in vacuum, at about 10 kPa, during 2 h at 90°C. PHB's chemical representation is  $(C_4H_6O_2)_n$  and its density is 1.2 g/cm<sup>3</sup> at room temperature. PHB has a relatively important molecular weight: 254 kg/mol. Dertoline was produced by DRT (France) in the form of flakes. Its molar mass is 1.1 kg/mol.

### 2.2 | Sample preparation

Neat PHB and PHB blends with 5, 10 or 15 wt% Dertoline were mixed using a mortar until a uniform and homogeneous powder was obtained. The blends of PHB and Dertoline are labeled PHB/Dertoline<sub>x</sub> or PHB/D<sub>x</sub> with the wt% of Dertoline as a subscript: *x*. Then, the powder was inserted in a twin-screw extruder (Minilab Thermo Scientific Haake) at 180°C, with a rotor speed of 60 rpm and retention time of 1 min. The extruded molten material was discharged into a microinjection unit (MiniJet Thermo Scientific Haake) at a pressure of 200 bars for 2 to 20 s, and the applied pressure was kept for another 2 to 20 s. The collector and the mold temperatures were set at 180 and 40°C, respectively. The injection pressure was adjusted according to the decrease of the polymer melt viscosity in order to obtain specimens of 60 × 20 × 1 mm.

### 2.3 | Instrumentation

The properties of the blends were tested using (i) differential scanning calorimetry (DSC), (ii) thermal gravimetry analysis (TGA), (iii) thermal dynamics mechanical analysis (DMA), (iv) polarized optical microscopy (POM), (v) uniaxial tensile testing, and (vi) rotational rheology.

DSC measurements were performed using the DSC25 and Q10 instruments from TA Instruments. To determine the melting and enthalpy temperature, a heating from –70°C to 200°C with a heating rate of 10°C/min was performed. The materials were first heated to 200°C, then cooled to –70°C quickly (100°C/min) and again heated to 200°C.

TGA was performed on a Setaram (Labsys EVO) instrument from room temperature to 600°C also at 10°C/min in air.

The dynamic thermal analyses (DMA) were conducted with a Q800 from TA instruments equipped with a liquid nitrogen cooler. Under a temperature range of -140°C to 170°C at 3°C/min and a frequency of 1 Hz, the samples were studied in tension mode with 0.07% deformation. The storage and loss modules as well as the loss factor for each sample were obtained as a function of temperature.

The samples were observed through POM using a Nikon Eclipse LV-N microscope, where the cross-section of thin films obtained from microtomic cutting were placed between cross-polarized light at room temperature.

Then, mechanical uniaxial tensile tests provided the modulus, strength, and failure strain. The materials samples were tested using an Instron 5965 Universal Testing Machine equipped with a cell load of 100 N according to the standard dimensions ASTM638. For each blend, 10 specimens were tested at a speed of 1 mm/min also at room temperature.

In addition, an ARES rheometer was used to study the viscoelastic properties of the samples. The rheometer is equipped with a forced convection oven and 25 mm diameter parallel plates. For each test the oven was preheated and then a sample disc was loaded in between the parallel plates and pressed to 0.9 mm. The temperatures were maintained for 20 seconds and the frequency sweep took 105 s.

## 3 | RESULTS AND DISCUSSION

### 3.1 | Thermal properties

In order to estimate the compatibility between the PHB and the Dertoline, DSC curves for PHB, PHB/Dertoline blends and Dertoline are shown in Figure 1. The samples experienced a first heating cycle, which is used to estimate the melting temperature,  $T_m$ , and the melting enthalpy,  $\Delta H_m$ . PHB has a clear melting peak, which is in contrast to the Dertoline which seems to have no clear melting in the range of temperature tested. The following cooling and melting cycles were used to estimate the glass transition temperatures,  $T_g$ . During cooling, cold crystallization peaks at temperature around 90°C for PHB/Dertoline blends are observed. Note a slight increase of the peak temperature for PHB/Dertoline<sub>10</sub> and a large decrease of the peak temperature for PHB/Dertoline<sub>15</sub> to 65°C. The increase could be explained by the presence of Dertoline which may act as a nucleating agent and PHB crystallization takes place

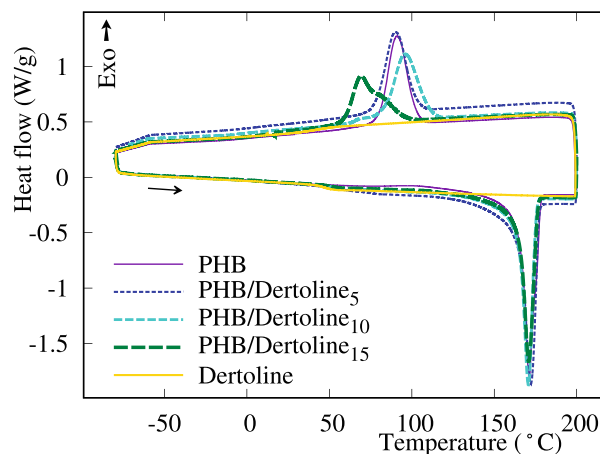


FIGURE 1 DSC curves of PHB, PHB/Dertoline and Dertoline samples from a heating and cooling thermal cycle at 10°C/min [Color figure can be viewed at [wileyonlinelibrary.com](http://wileyonlinelibrary.com)]

through a heterogeneous nucleating mechanism. The decrease in the peak temperature maybe due to confinement of polymer chains caused by the presence of Dertoline that prevent the diffusion and the migration of polymer chains. The thermal transition temperatures for PHB, Dertoline and the blends are listed in Table 1. The influence of the Dertoline on the melting temperature of the blends is small. Indeed, the melting temperature has practically no evolution after the addition of Dertoline. Nevertheless, the melting enthalpy experiences an increase for 5% Dertoline and then a decrease at 10%. Based on the DSC data, the degrees of crystallinity,  $\chi_c$ , can be calculated by the total enthalpy method with the following equation:

$$\chi_c = \frac{\Delta H_m}{W_{\text{PHB}} \Delta H_m^\circ} \times 100, \quad (1)$$

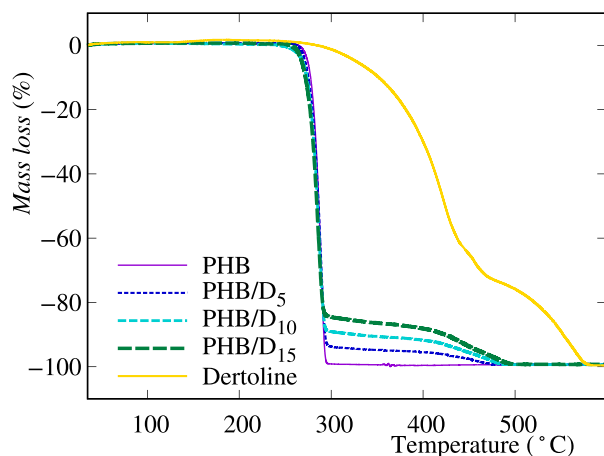
where  $\Delta H_m$  is the specific enthalpy of fusion of the samples studied,  $W_{\text{PHB}}$  is the mass amount of PHB in the mixture and  $\Delta H_m^\circ$  is the specific enthalpy of fusion of a 100% crystalline PHB with a value of 146 J/g.<sup>19</sup> The degrees of crystallinity of PHB and PHB/Dertoline are calculated taking into account the real amount of PHB in each sample and are also reported in Table 1. The theoretical  $T_g$  values of the blends were calculated with the Fox<sup>24</sup> equation:

$$\frac{1}{T_g} = \frac{w_1}{T_{g1}} + \frac{w_2}{T_{g2}}, \quad (2)$$

where subscripts  $w_1$  refers to weight fraction of the polymer (PHB) and  $w_2$  to the weight of plasticizer (Dertoline). Note, the  $T_g$  were calculated from the DSC

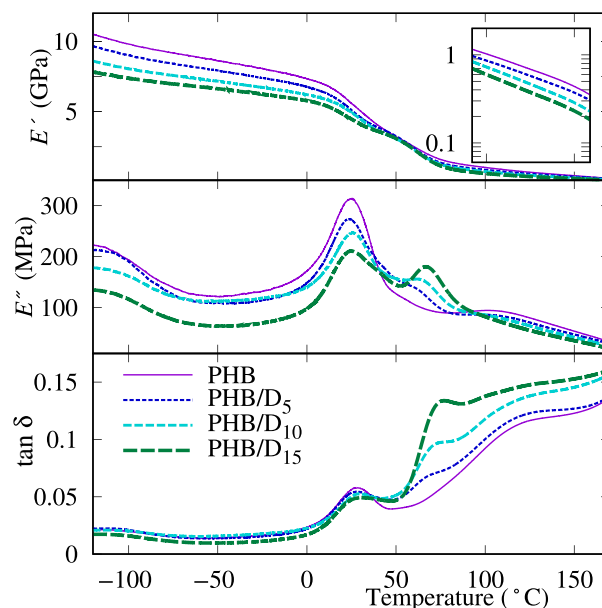
TABLE 1 Thermal transition DSC temperatures of PHB, PHB/Dertoline and Dertoline

Sample	Theoretical $T_g$ ( $^{\circ}\text{C}$ )	Experimental $T_g$ ( $^{\circ}\text{C}$ )	Experimental $T_m$ ( $^{\circ}\text{C}$ )	$\Delta H_m$ (J/g)	$\chi_c$ (%)
PHB	5	3.5	171.2	95.2	65.2
PHB/Dertoline <sub>5</sub>	7	3.8	172.2	101.1	72.9
PHB/Dertoline <sub>10</sub>	8.9	3.5	170.7	83.4	63.5
PHB/Dertoline <sub>15</sub>	10.5	3.7	170.9	80.2	64.6
Dertoline	50	43.8	–	–	–

FIGURE 2 TGA of PHB, PHB/Dertoline, and Dertoline sample at  $10^{\circ}\text{C}/\text{min}$  [Color figure can be viewed at [wileyonlinelibrary.com](https://onlinelibrary.wiley.com/doi/10.1002/app.53052)] 

data. For neat PHB and Dertoline,  $T_g$  are 5 and  $50^{\circ}\text{C}$ , respectively. The values of  $\chi_c$  and its dispersion are in good agreement with previous studies<sup>19,25</sup> where X-ray diffraction measurements of pure PHB have shown crystalline PHB macromolecules are packed in an orthorhombic unit cell that has a compact and a right-handed helix with screw axis. The effect of Dertoline terpene on the crystallinity of PHB/Dertoline blends is limited with a slight increase of  $\chi_c$ . The melting temperature of the PHB/Dertoline<sub>5</sub> remains unchanged compared to the neat PHB, but the crystallinity increases from 65.2% to 72.9%. This suggests that the addition Dertoline does not affect significantly the degree of crystallinity of the blends, but further studies are required to assess its effect on the size and orientation of the crystals.

TGA was conducted on the samples and is shown in Figure 2. The data for the blends show slight mass losses compared to neat PHB until  $270^{\circ}\text{C}$ . At  $280^{\circ}\text{C}$ , a sharp mass loss is observed and is due to the vaporization of the PHB. Then, in the range  $300$ – $400^{\circ}\text{C}$ , a small mass fraction of PHB (less than 20%) remains due to the slow vaporization of Dertoline. It is observed that the blends with largest Dertoline contents lose less weight. At  $500^{\circ}\text{C}$ , the PHB mass is null and only 24% of Dertoline is left, because of the complex aromatic compounds of

FIGURE 3 DMA of PHB and PHB/Dertoline samples at  $3^{\circ}\text{C}/\text{min}$  [Color figure can be viewed at [wileyonlinelibrary.com](https://onlinelibrary.wiley.com/doi/10.1002/app.53052)] 

Dertoline are most difficult to decompose. Finally, at  $600^{\circ}\text{C}$ , almost all the material is evaporated.

Figure 3 shows the DMA data over a temperature range from  $-110^{\circ}\text{C}$  to  $160^{\circ}\text{C}$ . It exhibits the usual large drop in storage modulus,  $E'$ , around  $20^{\circ}\text{C}$ . This decrease corresponds to a maximum value of the loss modulus  $E''$  and  $\tan\delta$ . A reduction of the maximum value of  $E''$  is observed with the increase Dertoline concentration. The peak is usually referred as the  $\alpha$ -relaxation, also observed in X-ray diffraction,<sup>19</sup> and is not shifted horizontally by the presence of Dertoline. But, at elevated temperatures, interactions between PHB and Dertoline lead to additional peaks of  $E''$  and  $\tan\delta$ . It suggests the Dertoline properties are enhancing the material properties in comparison to the neat PHB. Note that for temperature above  $60^{\circ}\text{C}$ , the storage module  $E'$  diminishes with the Dertoline content.

POM images are shown in Figure 4 and represent the microstructure of the PHB and PHB/Dertoline material, which was rapidly cooled to room temperature after microinjection. The main features of the POM images is



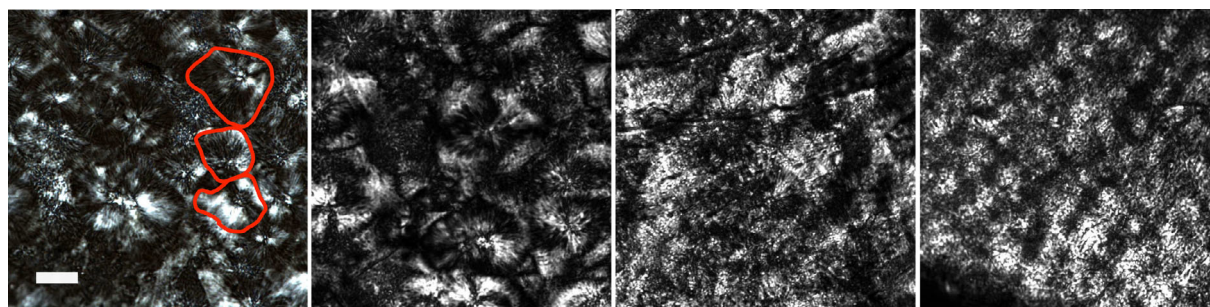


**FIGURE 4** POM observation of the PHB, PHB/Dertoline<sub>5</sub>, PHB/Dertoline<sub>10</sub>, PHB/Dertoline<sub>15</sub> (from left to right) at room temperature. The red lines represent spherulitic crystalline structures and the scale bar represents 20  $\mu\text{m}$ . [Color figure can be viewed at [wileyonlinelibrary.com](http://wileyonlinelibrary.com)]

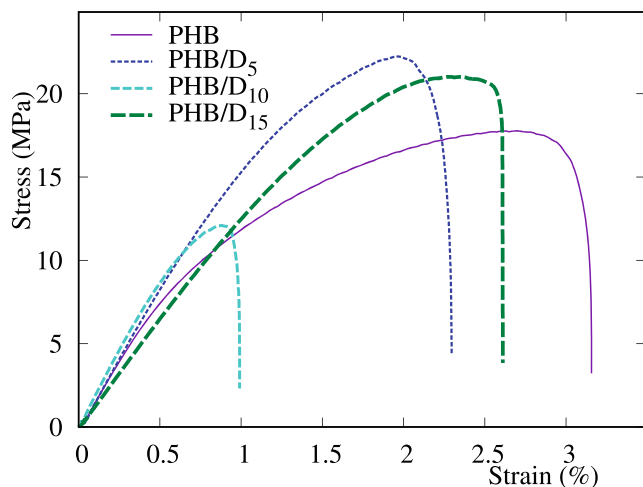


**FIGURE 5** Strain and stress curves of PHB and PHB/Dertoline [Color figure can be viewed at [wileyonlinelibrary.com](http://wileyonlinelibrary.com)]

the appearance of spherulites with first a slight increase of average diameter and then a decrease of diameter with the increase of Dertoline content. In blends of PHB and other plasticizers such as talc,<sup>26</sup> glycerol, tributyrin, triacetin,<sup>27</sup> starch,<sup>28</sup> or triethyl citrate,<sup>29</sup> previous investigations have also reported an effect on the nucleation density and growth rate of spherulite.<sup>30,31</sup> Moreover, the presence of spherulite crystals is associated to intraspherulitic cracks that are known to appear either in radial or circumferential direction within the spherulites depending on the crystallization temperature<sup>25,32</sup> and cause brittleness. The natural plasticizer (Dertoline) added here into the PHB polymer acts as a nucleation agent modifying the density of the nuclei.

### 3.2 | Mechanical properties

The mechanical traction test results at room temperature are presented in the form of stress–strain curves in

**TABLE 2** Mechanical properties of PHB and PHB/Dertoline

Sample	$E$ (MPa)	$\sigma_r$ (MPa)	$\epsilon_r$ (%)
PHB	$1508 \pm 232$	$11 \pm 7$	$2.8 \pm 1.5$
PHB/Dertoline <sub>5</sub>	$1859 \pm 546$	$12 \pm 7$	$2.4 \pm 0.7$
PHB/Dertoline <sub>10</sub>	$1849 \pm 191$	$10 \pm 7$	$1.4 \pm 0.6$
PHB/Dertoline <sub>15</sub>	$1316 \pm 140$	$17 \pm 7$	$2.3 \pm 0.7$

Figure 5 and summarized in Table 2. It is observed that the incorporation of 5 wt % of Dertoline caused an increase in the Young's modulus from 1508 MPa for the neat matrix to 1859 MPa. Then, the decrease is more significant as the content of Dertoline increases and  $E$  reduces by 14% for the highest Dertoline content. For the stress at the break ( $\sigma_r$ ) and the strain at break ( $\epsilon_r$ ), the trend remain unclear and the changes are not significant. It is interesting to note that PHB evolves as a brittle material in the long term because of a relatively high crystallinity and in particular the significant secondary crystallization that occurs while aging.<sup>25</sup> An alternative approach to circumvent the compatibility and the brittleness of PHB materials is to consider copolymers.<sup>33</sup>

### 3.3 | Viscoelastic properties

Oscillatory measurements were performed in the linear viscoelastic regime with 1% strain amplitude. The oscillatory frequency was limited from 100 to 1 rad/s in order to limit the duration of each test. Multiple runs were carried out with a new sample at different temperatures:  $T = 168, 172, 174, 176, 178,$  and  $180^\circ\text{C}$ . The results were combined using the time temperature superposition at a reference temperature of  $168^\circ\text{C}$  using the REPTATE rheology software.<sup>34</sup> Figure 6a presents the storage modulus,  $G'$ , the loss modulus,  $G''$ , and the complex viscosity,  $\eta^* = \sqrt{G'^2 + G''^2}/\omega$ , as a function of the reduced angular velocity  $a_T\omega$ , where  $a_T$  are the shifting factors.

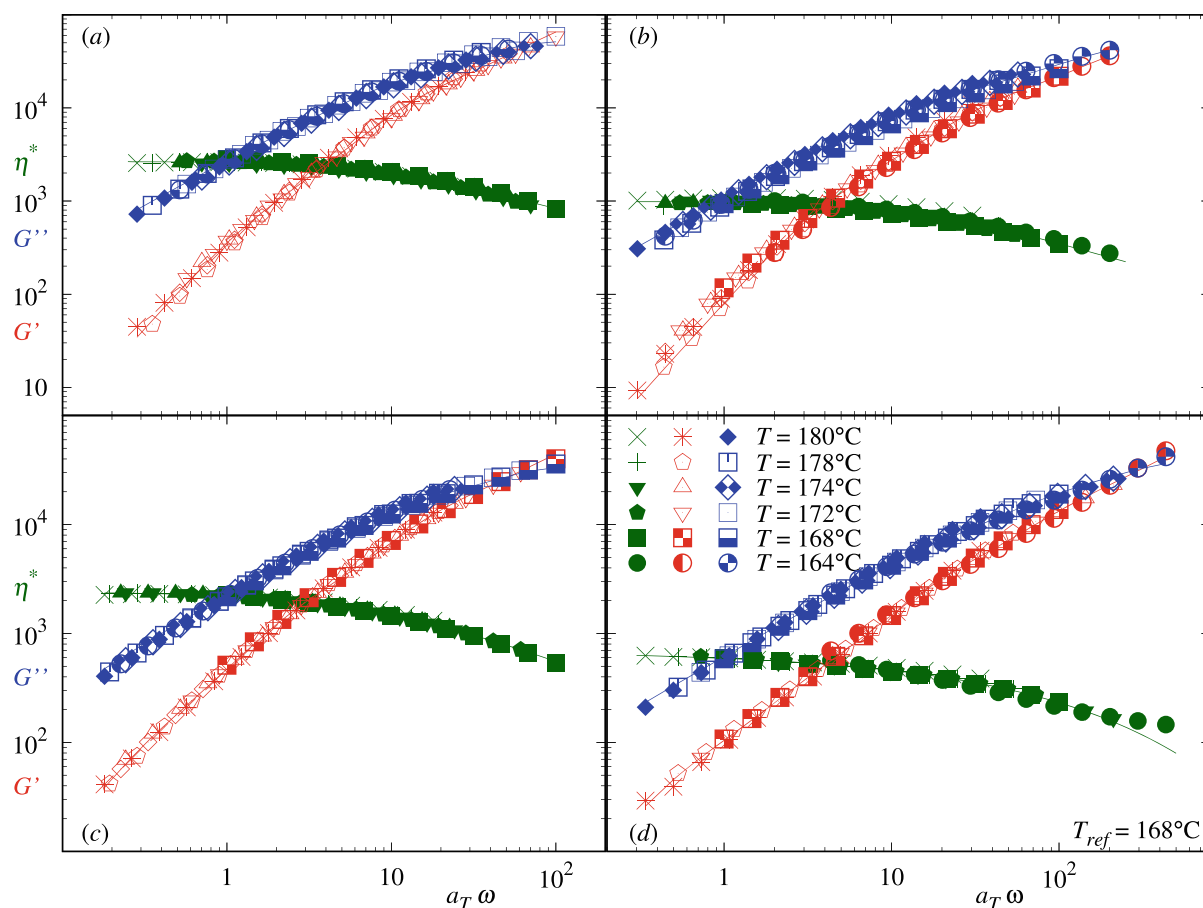


**FIGURE 6** Dynamic moduli ( $G'$  and  $G''$ ) and complex viscosity ( $\eta^*$ ) as a function of shifted angular frequency ( $a_T \omega$ ) at a reference temperature  $T_{ref} = 168^\circ\text{C}$  for (a) PHB, (b) PHB/Dertoline<sub>5</sub>, (c) PHB/Dertoline<sub>10</sub>, and (d) PHB/Dertoline<sub>15</sub>. The lines are the Maxwell and Cross models described in the text with the parameters listed in Tables 3 and 4 [Color figure can be viewed at [wileyonlinelibrary.com](http://wileyonlinelibrary.com)]

For PHB/Dertoline blends, the behavior of  $G'$  and  $G''$  are essentially similar to PHB, as seen in Figure 6(b-d). Yet, the plateau of the complex viscosity,  $\eta^*$ , seems to decrease with the concentration of Dertoline. This variation illustrates the large variability of the sample properties. The behavior of  $\eta^*$  of the PHB and PHB/Dertoline can be modeled using a modified Carreau–Yasuda model:

$$|\eta^*(\omega)| = \eta_0 [1 + (\omega\lambda)^a]^{\frac{n-1}{a}} \quad (3)$$

The parameters the Carreau–Yasuda fits are given in Table 3 and indicate no clear monotonous behavior of the shear-thinning index ( $n$ ). The characteristic relaxation time ( $\lambda$ ) from the Carreau–Yasuda fit varies from 21 to 97 ms. Another relaxation time can be defined by the crossing between the moduli that leads to  $1/\omega_c \simeq 0.5$  s at  $T = 164^\circ\text{C}$ . Clearly, the whole polymer melt cannot be represented by a single relaxation time.

**TABLE 3** Parameters of the modified Carreau–Yasuda model for PHB and PHB/Dertoline

	$\eta_0$ (Pa s)	$n$	$\lambda$ (ms)
PHB	2648	0.94	29
PHB/Dertoline <sub>5</sub>	986	1.07	21
PHB/Dertoline <sub>10</sub>	2782	0.82	97
PHB/Dertoline <sub>15</sub>	646	0.86	28

The actual relaxation of a polymer chain has a spectrum of relaxation times. This can be represented with the generalized Maxwell model:

$$G'(\omega) = \sum_{i=1}^N \frac{G_i(\omega\lambda_i)^2}{1 + (\omega\lambda_i)^2} \quad (4)$$

$$G''(\omega) = \sum_{i=1}^N \frac{G_i(\omega\lambda_i)}{1 + (\omega\lambda_i)^2} \quad (5)$$

**TABLE 4** Parameters of the generalized Maxwell model for PHB and PHB/Dertoline

	$i$	$G_i$ (Pa)	$\lambda_i$ (s)
PHB	1	282.7	0.958
	2	5314.8	0.179
	3	31,220.3	0.034
	4	95,568.3	0.006
PHB/Dertoline <sub>5</sub>	1	726.2	0.339
	2	9637.4	0.049
	3	31,408.4	0.007
	4	116,817	0.001
PHB/Dertoline <sub>10</sub>	1	134.6	2.691
	2	2189.5	0.394
	3	16,743.3	0.058
	4	61,692.6	0.008
PHB/Dertoline <sub>15</sub>	1	87.0	1.649
	2	1089.1	0.183
	3	11,536	0.020
	4	64,753.3	0.002

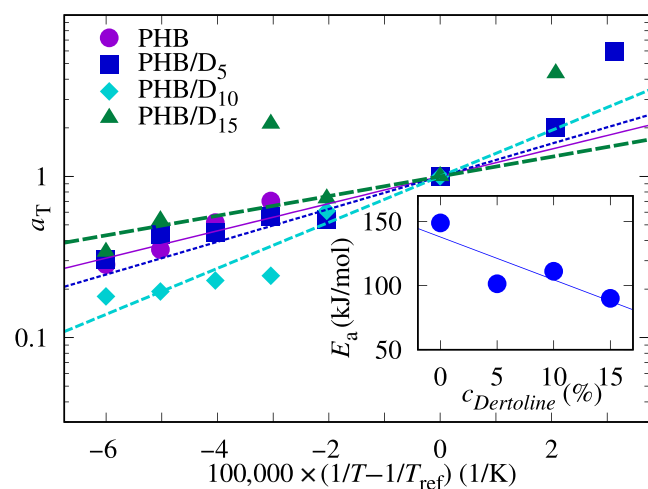


**FIGURE 7** Shift factor,  $a_T$ , as a function of  $1/T - 1/T_{\text{ref}}$  for PHB and PHB/Dertoline.  $T_{\text{ref}}$  is  $168^\circ\text{C}$  and the lines are linear fits. The inset is the activation energy,  $E_a$ , as a function of the weight ratio of Dertoline in PHB [Color figure can be viewed at [wileyonlinelibrary.com](https://onlinelibrary.wiley.com)]

where  $G_i$  and  $\lambda_i$  are the modulus and relaxation time corresponding to the  $i$ th Maxwell element of the generalized Maxwell model. The measured  $G'$  and  $G''$  are fitted by four Maxwell elements, which are represented by lines in

Figure 6 and the parameters are listed in Table 4. Four elements are sufficient to describe the viscoelastic behavior, which is viscous dominated before the crossing point.

From the time–temperature superposition, the shift factors,  $a_T$ , are presented in Figure 7 as a function of  $1/T - 1/T_{\text{ref}}$ . Close to the  $T_g$ , the thermal dependency of  $a_T$  is usually described by the Williams-Landel-Ferry (WLF) equation.<sup>35</sup> However, here at higher temperature, the free volume is no longer the limiting factor and the viscosity-temperature relationship follows an Arrhenius equation<sup>36</sup>:

$$\ln a_T = E_a/R \times (1/T - 1/T_{\text{ref}}) \quad (6)$$

where  $E_a$  is the apparent activation energy linked to the energy needed for a chain segment to jump between an occupied site and an unoccupied one.  $R$  is the gas constant and  $T_{\text{ref}}$  is the reference temperature, here  $T_{\text{ref}} = 168^\circ\text{C}$ . In the inset of Figure 7,  $E_a$  is plotted as a function of the weight fraction of Dertoline in PHB, the values are in a range of 150 to 50 kJ/mol and decreases with percentage of Dertoline. Previous estimates of the  $E_a$  for PHB<sup>37</sup> are in the range 37–40 kJ/mol. The present high values of  $E_a$  indicate a rapid variation of the thermo-rheological properties of PHB and PHB blends.

### 3.4 | Transient rheology

The previous viscoelastic data were obtained after few minutes at temperatures close to the melting temperature. In order to estimate the degradation time associated with PHB and PHB/Dertoline, transient tests have been performed from 0 to 600 s at different temperatures from  $174$  to  $186^\circ\text{C}$ . Figure 8 presents the results for oscillatory tests in terms of relative viscosity, which is the ratio of the viscosity at a given time and the viscosity at  $t = 0$ . The oscillations are stress controlled with amplitude of 1% and frequency of 1 rad/s. In Figure 8a, one can propose there is a plateau between 0 and 120 s for the temperatures under  $180^\circ\text{C}$  where relative viscosity remains roughly constant. That is why we operate in this short amount of time (120 s) for our dynamic frequency sweep presented earlier. The polymer was strongly degraded in a short amount of time, 40% in 200 s, independently of the temperature. Shear measurements at  $10 \text{ s}^{-1}$  were not possible as the sample does not remain between the plates. For PHB/Dertoline<sub>5</sub>, Figure 8b presents the transient oscillatory tests, where there is a bigger fall of relative viscosity between 0 and 100 s. For PHB/Dertoline<sub>10</sub> and PHB/Dertoline<sub>15</sub>, the decrease of relative viscosity between 0 and 100 s is not improved compared to neat PHB.



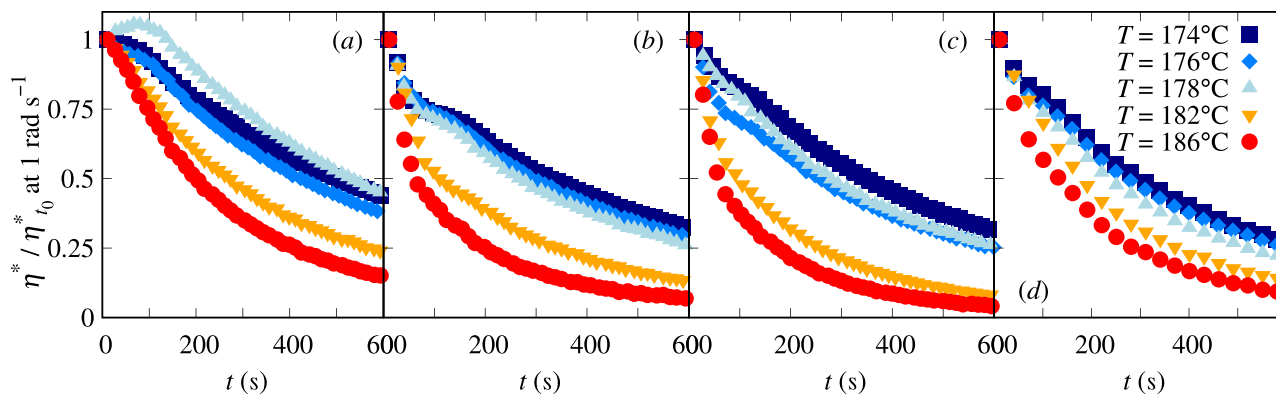


FIGURE 8 Transient relative viscosity of oscillatory tests for (a) PHB, (b) PHB/Dertoline<sub>5</sub>, (c) PHB/Dertoline<sub>10</sub>, and (d) PHB/Dertoline<sub>15</sub> at different temperatures [Color figure can be viewed at [wileyonlinelibrary.com](http://wileyonlinelibrary.com)]

## 4 | CONCLUSION

In conclusion, biobased and biodegradable PHB/Dertoline blends have been examined through POM, DSC, TGA, DMA, and tensile tests. The addition of Dertoline first increases the degree of crystallinity from DSC at 5 wt% Dertoline and then decreases slightly the crystallinity, compared to neat PHB. TGA suggests an augmented thermal stability with the addition of Dertoline. Moreover, smaller spherulites are observed for 10 and 15% Dertoline samples, which results in larger measured strains at break. In addition, transient oscillatory rheology at different temperatures indicate the degradation is slightly prevented at low temperature 170°C. Overall, the rapid reduction of polymer melt viscosity at high temperature only allows to process PHB for a short running time. Hence, the PHB is recommended for micro-screw extrusion for example in additive manufacturing, such as fused deposited modeling technologies.<sup>38</sup> Finally, the temperature rheology time superposition was obtained so that activation energies and parameters of the Carreau-Yasuda and Maxwell models are provided, which could be used to model precisely the melt flow behavior. In the future, more properties of the blend need to be quantified: the aging, the antioxidant effects, the gas permeability,<sup>39</sup> the crystalline structure,<sup>40</sup> the flammability and the cost effectiveness and life cycle.<sup>41,42</sup>

### AUTHOR CONTRIBUTIONS

**Gaëtan Charon:** Data curation (equal); investigation (equal); validation (equal); writing – original draft (equal). **Jorge Peixinho:** Conceptualization (equal); data curation (equal); formal analysis (lead); methodology (equal); software (lead); supervision (equal); visualization (lead); writing – original draft (equal); writing – review and editing (lead). **Laurent Michely:** Data curation (equal); methodology (equal); resources (equal); writing – review and editing (supporting). **Alain Guinault:**

Conceptualization (lead); formal analysis (lead); funding acquisition (lead); investigation (equal); methodology (equal); project administration (lead); resources (lead); writing – review and editing (supporting). **Valérie Langlois:** Conceptualization (lead); formal analysis (equal); funding acquisition (lead); project administration (lead); resources (equal); supervision (equal); writing – review and editing (supporting).

### ACKNOWLEDGMENTS

Valérie Langlois thanks Estelle Renard for suggesting the Dertoline as a plasticizer. The authors thank Béatrice Huynh for assistance in the initial experiments and our colleagues Cathia Farra and Gilles Régner for useful discussions. Financial support from ANR PRCI SEABIOP is acknowledged.

### DATA AVAILABILITY STATEMENT

The data that support the findings of this study are available from the corresponding author upon reasonable request.

### ORCID

Jorge Peixinho  <https://orcid.org/0000-0003-0850-3406>

Laurent Michely  <https://orcid.org/0000-0001-8785-6191>

### REFERENCES

- [1] A. Steinbüchel, H. E. Valentin, *FEMS Microbiol. Lett.* **1995**, *128*, 219.
- [2] K. Sudesh, H. Abe, Y. Doi, *Prog. Polym. Sci.* **2000**, *25*, 1503.
- [3] R. W. Lenz, R. H. Marchessault, *Biomacromolecules* **2005**, *6*, 1.
- [4] Y. Tokiwa, B. P. Calabia, *Biotechnol. Lett.* **2004**, *26*, 1181.
- [5] E. Renard, M. Walls, P. Guérin, V. Langlois, *Polym. Degrad. Stab.* **2004**, *85*, 779.
- [6] K. Numata, H. Abe, T. Iwata, *Materials* **2009**, *2*, 1104.
- [7] P. Guérin, E. Renard, V. Langlois, in *Plastics from Bacteria: Natural Functions and Applications*, Microbiology Monographs

- (Ed: G.-Q. Chen), Springer-Verlag, Berlin Heidelberg **2010**, p. 283.
- [8] T. G. Volova, S. V. Prudnikova, O. N. Vinogradova, D. A. Syrvacheva, E. I. Shishatskaya, *Microb. Ecol.* **2017**, *73*, 353.
- [9] R. Rai, T. Keshavarz, J. A. Roether, A. R. Boccaccini, I. Roy, *Mater. Sci. Eng. R Rep.* **2011**, *72*, 29.
- [10] J. Zhang, E. I. Shishatskaya, T. G. Volova, L. F. da Silva, G.-Q. Chen, *Mater. Sci. Eng. C* **2018**, *86*, 144.
- [11] M. Koller, *Molecules* **2018**, *23*, 362.
- [12] M. Auriemma, A. Piscitelli, R. Pasquino, P. Cerruti, M. Malinconico, N. Grizzuti, *Eur. Polym. J.* **2015**, *63*, 123.
- [13] I. Roy, P. M. Visakh, *Polyhydroxyalkanoate (PHA) Based Blends, Composites and Nanocomposites*, Royal Society of Chemistry, Cambridge, UK **2014**.
- [14] J. S. Choi, W. H. Park, *Polym. Test.* **2004**, *23*, 455.
- [15] M. G. A. Vieira, M. A. da Silva, L. O. dos Santos, M. M. Beppu, *Eur. Polym. J.* **2011**, *47*, 254.
- [16] D. Garcia-Garcia, J. M. Ferri, N. Montanes, J. Lopez-Martinez, R. Balart, *Polym. Int.* **2016**, *65*, 1157.
- [17] M. J. Jenkins, A. V. L. Fitzgerald, C. A. Kelly, *Polym. Degrad. Stab.* **2019**, *159*, 116.
- [18] L. F. Longé, L. Michely, A. Gallos, A. Rios De Anda, H. Vahabi, E. Renard, M. Lacroche, F. Allais, V. Langlois, *Bioengineering* **2022**, *9*, 100.
- [19] C. Mangeon, L. Michely, A. R. de Anda, F. Thevenieau, E. Renard, V. Langlois, *ACS Sustain. Chem. Eng.* **2018**, *6*, 16160.
- [20] M. Kanerva, A. Puolakka, T. M. Takala, A. M. Elert, V. Mylläri, I. Jönkkäri, E. Sarlin, J. Seitsonen, J. Ruokolainen, P. Saris, J. Vuorinen, *Mater. Today Commun.* **2019**, *20*, 100527.
- [21] H. Moustafa, N. E. Kissi, A. I. Abou-Kandil, M. S. A.-A. Mohamed, A. Dufresne, *ACS Appl. Mater. Interfaces* **2017**, *9*, 20132.
- [22] M. Kaavessina, S. Distantina, A. Chafidz, A. Utama, V. M. P. Anggraeni, *AIP Conference Proceedings*, Vol. 2018, AIP Publishing LLC, Surakarta, Indonesia **1931**, 030006.
- [23] H. D. L. Rosa-Ramírez, M. Aldas, J. M. Ferri, J. López-Martínez, M. D. Samper, *J. Appl. Polym. Sci.* **2020**, *137*, 49346.
- [24] T. Fox, *Bull. Am. Phys. Soc.* **1956**, *1*, 123.
- [25] B. Laycock, P. Halley, S. Pratt, A. Werker, P. Lant, *Prog. Polym. Sci.* **2013**, *38*, 536.
- [26] Y. Inoue, N. Yoshie, *Prog. Polym. Sci.* **1992**, *17*, 571.
- [27] A. El-Hadi, R. Schnabel, E. Straube, G. Müller, S. Henning, *Polym. Test.* **2002**, *21*, 665.
- [28] R. M. S. M. Thiré, T. A. A. Ribeiro, C. T. Andrade, *J. Appl. Polym. Sci.* **2006**, *100*, 4338.
- [29] L. V. Scalioni, M. C. Gutiérrez, M. I. Felisberti, *J. Appl. Polym. Sci.* **2017**, *134*, 14.
- [30] P. Xu, C. Zhang, G. Qi, W. Yang, P. Ma, *J. Polym. Res.* **2022**, *29*, 1.
- [31] J. Chen, C. Xu, D. Wu, K. Pan, A. Qian, Y. Sha, L. Wang, W. Tong, *Carbohydr. Polym.* **2015**, *134*, 508.
- [32] P. J. Barham, A. Keller, *J. Polym. Sci. B Polym. Phys.* **1986**, *24*, 69.
- [33] M. Boufarguine, A. Guinault, G. Miquelard-Garnier, C. Sollogoub, *Macromol. Mater. Eng.* **2013**, *298*, 1065.
- [34] V. A. Boudara, D. J. Read, J. Ramirez, *J. Rheol.* **2020**, *64*, 709.
- [35] J. D. Ferry, *Viscoelastic Properties of Polymers*, John Wiley & Sons, Inc, New York **1980**.
- [36] I. M. Ward, D. W. Hadley, *An Introduction to the Mechanical Properties of Solid Polymers*, Wiley, Chichester, UK **1993**.
- [37] Q. Liao, I. Noda, C. W. Curtis, *Polymer* **2009**, *50*, 6139.
- [38] J. Tian, R. Zhang, Y. Wu, P. Xue, *Mater. Des.* **2021**, *199*, 109418.
- [39] G. Miquelard-Garnier, A. Guinault, C. Sollogoub, M. Gervais, *Express Polym Lett* **2018**, *12*, 114.
- [40] P. N. Tri, S. Domenek, A. Guinault, C. Sollogoub, *J. Appl. Polym. Sci.* **2013**, *129*, 3355.
- [41] E. Bugnicourt, P. Cinelli, A. Lazzeri, V. A. Alvarez, *Express Polym Lett* **2014**, *8*, 791.
- [42] J. K. Muiruri, J. C. C. Yeo, Q. Zhu, E. Ye, X. J. Loh, Z. Li, *ACS Sustain. Chem. Eng.* **2022**, *10*, 3387.

**How to cite this article:** G. Charon, J. Peixinho, L. Michely, A. Guinault, V. Langlois, *J. Appl. Polym. Sci.* **2022**, *139*(43), e53052. <https://doi.org/10.1002/app.53052>